Environmental Pollution 232 (2018) 310–321

Contents lists available at ScienceDirect

Environmental Pollution

journal homepage: www.elsevier.com/locate/envpol

Realtime chemical characterization of post monsoon organic aerosols in a polluted urban city: Sources, composition, and comparison with other seasons☆

Abhishek Chakraborty [a, 1], Anil Kumar Mandariya [a], Ruparati Chakraborti [a], Tarun Gupta [a, b, *], S.N. Tripathi [a, b]

[a] Department of Civil Engineering, Indian Institute of Technology, Kanpur, India
[b] Centre of Environmental Science and Engineering, CESE, IIT Kanpur, India

ARTICLE INFO

Article history:
Received 2 April 2017
Received in revised form
10 August 2017
Accepted 25 September 2017
Available online 30 September 2017

Keywords:
Organic aerosols
Oxidation
Sources
Seasonal variations
Post monsoon

ABSTRACT

Real time chemical characterization of non-refractory submicron aerosols (NR-PM_1) was carried out during post monsoon (September–October) via Aerosol Mass Spectrometer (AMS) at a polluted urban location of Kanpur, India. Organic aerosol (OA) was found to be the dominant species with 58% contribution to total NR-PM_1 mass, followed by sulfate (16%). Overall, OA was highly oxidized (average O/C = 0.66) with the dominance of oxidized OAs (60% of total OA) as revealed by source apportionment. Oxidized nature of OA was also supported by very high OC/EC ratios (average = 8.2) obtained from simultaneous offline filter sampling. High and low OA loading periods have very dramatic effects on OA composition and oxidation. OA O/C ratios during lower OA loading periods were on average 30% higher than the same from high loading periods with significant changes in types and relative contribution from oxidized OAs (OOA). Comparison of OA sources and chemistry among post monsoon and other seasons revealed significant differences. Characteristics of primary OAs remain very similar, but features of OOAs showed substantial changes from one season to another. Winter had lowest OOA contribution to total OA but similar overall O/C ratios as other seasons. This reveals that processing of primary OAs, local atmospheric chemistry, and regional contributions can significantly alter OA characteristics from one season to another. This study provides interesting insights into the seasonal variations of OA sources and evolution in a very polluted and complex environment.

1. Introduction

Submicron size aerosols are an integral part of Earth's atmosphere with significant impacts (direct and indirect) on human health, global climate, and visibility. A large fraction (20–80%) of ambient fine size aerosols is made up of organic aerosols (OA) (Ervens et al., 2011; Hallquist et al., 2009; Jimenez et al., 2009; Ng et al., 2011). Nature of OA can be both primary and secondary, with primary OA (POAs) being directly emitted via biomass burning (BB), volcanic eruptions, fossil fuel combustion, and sea spray. Atmospheric oxidation of VOCs by radicals and oxidants like OH, NO_3, O_3 and subsequent partitioning of gas phase oxidation products into particulate phase lead to the formation of secondary OA (SOA). Additional SOA can be produced via heterogeneous reactions in cloud/fog droplets and over particulate surface (Ervens et al., 2011; Hallquist et al., 2009). Characterization and evaluation of OA properties are quite challenging because of their different emission sources, variations in atmospheric processing, meteorological factors, differences in physico-chemical properties (solubility, volatility, optical properties, etc.) and long range transport. These spatio-temporal variations make OA characterization a difficult task and lead to inaccurate assessment of its impact on regional climate (Hallquist et al., 2009). Also, the scale of atmospheric processing is rather short thus offline filter based methods with 8–12 h time resolution are inadequate to capture the evolution of OA characteristics. Fortunately, recent advances made in mass spectrometry and the arrival of Aerosol Mass Spectrometers has offered some detailed and unique insights into OA composition, chemistry, characteristics and their temporal evolution. Aerodyne High

☆ This paper has been recommended for acceptance by Baoshan Xing.
* Corresponding author. Department of Civil Engineering, Indian Institute of Technology, Kanpur, India.
E-mail addresses: tarun@iitk.ac.in (T. Gupta), snt@iitk.ac.in (S.N. Tripathi).
[1] Now at IMT Lille Douai, SAGE, 59500 Douai, France.

https://doi.org/10.1016/j.envpol.2017.09.079
0269-7491/

Resolution-Aerosol Mass Spectrometer (HR-ToF-AMS, from now on termed as AMS) (Canagaratna et al., 2007; DeCarlo et al., 2006; Drewnick et al., 2005) is one such widely used instrument, capable of real time characterization of non-refractory submicron aerosols. Utilizing AMS data, one can obtain real time changes occurring in elemental ratios (O/C, H/C, OM/OC) of OA via atmospheric processing, which in turn can provide valuable information about OA evolution and characteristics. By applying additional source apportionment tools like Positive Matrix Factorization (PMF) even further information about OA sources and composition can be obtained. In India, most of the studies conducted till now are offline filter based studies which provided no or insufficient information on OA sources, composition and temporal evolution (Chakraborty and Gupta, 2010; Kaul et al., 2011; Rajput and Sarin, 2014; Ram et al., 2014). Indo Gangetic Plain (IGP) is one of the world's most densely populated region (Bhattu and Tripathi, 2015; Chakraborty et al., 2015; Kaul et al., 2011) with half of India's population residing here. Several major populated and polluted cities are located in IGP and Kanpur is one of them. Very recently, a few AMS based studies (Bhattu and Tripathi, 2015; Chakraborty et al., 2016b, 2015) have been conducted in IGP which showed the dominance of OA in submicron aerosols and provided new insights into OA evolution. However, those studies were mostly carried out during winter thus unable to provide seasonal characteristics, chemistry, and composition of OA. To devise an effective mitigation strategy for severe air pollution in IGP region, a holistic picture of OA with seasonal characteristics and sources is desired. Hence, it is imperative to understand the seasonal characteristics and chemistry of OA at this location, hitherto unknown for the IGP. This study is reporting for the first time the post monsoonal characteristics and sources of OA via real time measurements. A comparison with monsoon and winter time aerosol characteristics also provides some much needed insight into the changes in OA composition and characteristics from one season to another.

2. Materials and methods

2.1. Sampling site and sampling protocols

The sampling site (Fig. 1) is in the campus of Indian Institute of Technology (IIT), located at Kanpur (26.30 °N; 80.14 °E, 142 m above mean sea level: amsl) in the state of Uttar Pradesh (central part of IGP). The sampling site is located away from city center but within city limits. It's an academic campus with lots of greenery and away from industrial areas. Majority of the campus residents' use bicycles although a low volume traffic coming from outside is mainly comprised of two and four wheelers. Both, online and offline sampling was carried out during September–October. Ambient temperature during sampling period varied from 16 to 36 °C and relative humidity was ~50% at the sampling site. Real time AMS measurements of non-refractory submicron aerosols (NR-PM_1) have been carried out with a 2 min time resolution in high sensitivity V mode. Briefly, the AMS samples ambient air through a 100 μm diameter critical orifice and then focus particles through a series of aerodynamic lenses. A chopper wheel then delivers a slug of particles into the vacuum region of time of flight segment, wherein they attain distinct velocity proportional to their size. Subsequently, focused particles are subjected to vaporization using heated tungsten surface maintained at 600 °C in high vacuum (pressure around 10^{-8} Torr). Once in contact with the vaporizer, volatile and semi-volatile contents of the aerosol are flash vaporized (within a few seconds) followed by ionization via electron bombardment from AMS filament. This is a hard ionization process called hard electron impact (ionization energy = 70 eV). Ionized molecules are then analyzed by Time of Flight mass spectrometry. Transmission efficiency of aerodynamic lenses is almost 100% for spherical particles with vacuum aerodynamic diameters (D_{va}) between 60 nm and 700 nm. More details about AMS working principles and uncertainties can be found elsewhere (Canagaratna et al., 2007; DeCarlo et al., 2006; Drewnick et al., 2005).

AMS can measure non-refractory submicron aerosol species like organics, sulfate, nitrate, chloride, and ammonium in real time. High resolution data of AMS can provide even more detailed information on OA chemistry and composition. High resolution (HR) data is processed using PIKA (v1.10H) in IgorPro. Although AMS allows real time aerosol characterization, it has some limitations. Due to hard ionization, molecular identities of organic components are completely lost. AMS can only detect non-refractory part of submicron aerosols due to 600 °C vaporization temperature. Thus, important refractory organic materials such as EC can't be characterized via AMS. AMS also can't perform single particle analysis and it is essentially a bulk characterization instrument. Quantitative data accuracy of AMS depends on chosen collection efficiency (CE) value, which accounts for the aerosol loss during transmission through aerodynamic lenses and bouncing off from vaporizer. CE value is calculated using a literature (Middlebrook et al., 2012) based formulation which takes aerosol chemical composition in consideration. The calculation revealed a value of 0.5, which has been previously used in the majority of the field campaigns around the world, and this value has also been found satisfactory for this location in our previous AMS based studies (Bhattu and Tripathi, 2015; Chakraborty et al., 2015). Choice of CE value is further justified by the good correlation obtained between offline OC and AMS OM values (Fig. S1), with a slope almost equal to the OM/OC ratio determined from AMS HR analysis (described in the next section).

Hybrid Single-Particle Lagrangian Integrated Trajectory (HYSPLIT4) model developed by NOAA/Air Resources Laboratory (ARL) (Draxler and Rolph, 2003) was used to perform back trajectory (BT) analysis. The meteorological data required for the trajectory computation come from the Global Data Assimilation System archive maintained by ARL (available online at http://ready.arl.noaa.gov/archives.php). First, 78 h back trajectories were calculated at 500 m above the ground at every hour throughout the study period. Next, clustering of the trajectories were done as per spatial distributions using HYSPLIT4 software. The principles and processes associated with clustering are described in the software user guide (Draxler et al., 2014). Potential Source Contribution Function (PSCF) analysis was carried out utilizing BT analysis and using a tool called Zefir (V 3.321). Detail description of this tool can be found in previous studies (Petit et al., 2017; Zhang et al., 2017).

Offline PM_1 (particulate matter with aerodynamic diameter $\leq$ 1 μm) sampling has been carried out using a medium-volume air-sampler (calibrated flow-rate 175 l/min) (Kumar and Gupta, 2015). The samples were collected during day time for 45 min each (n = 119 and 10 blanks) onto pre-baked (at 600 °C for 8 h) quartz fiber filters (Whatman™; 47 mm Dia). Quartz filters were used as characterization of organic aerosols was the focus of this study, and in future, we intend to carry out a detail offline characterization study of the organics in collected filters. The short duration of the sampling was chosen to have some parity with the high time resolved sampling of AMS. Also, shorter duration sampling enabled us to have more number of filters and reduce the influence of sampling artifacts (like flow fluctuations, absorption of gas phase organics by filters) on observed concentrations. However, this high frequency sampling schedule demanded constant availability of alert manpower and a huge number of costly filters. Night time sampling was difficult due to limited availability of manpower and some short lasting but relatively frequent power cuts. So, considering logistical and economic aspects, only daytime high

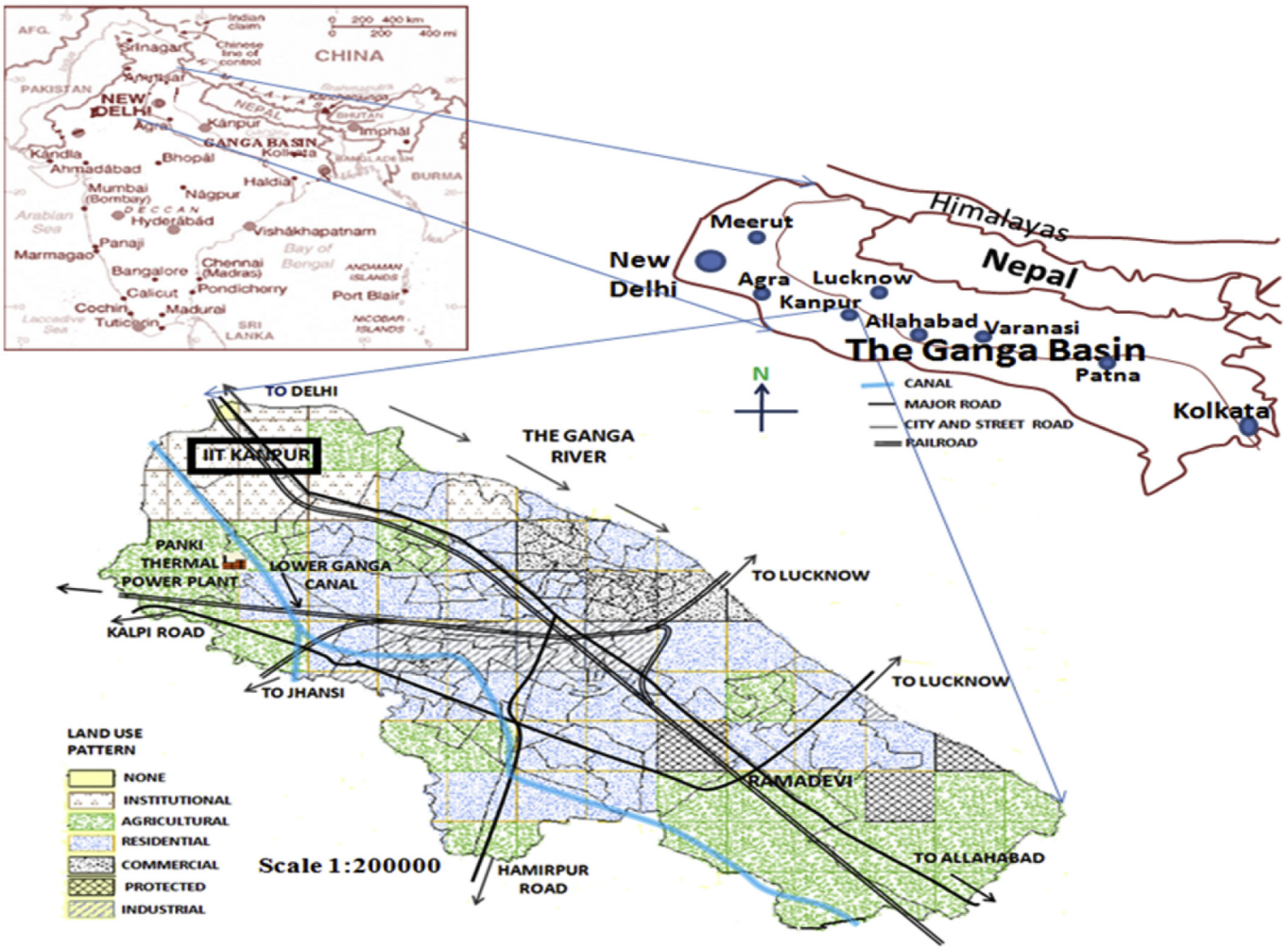

Fig. 1. Map of the Kanpur city and the study site (in black box).

frequency sampling was carried out. A portion of each aerosol-laden filter was analyzed in offline Sunset Lab EC/OC analyzer to obtain OC and EC values (Kaul et al., 2011).

OC and EC are measured in Thermal-Optical-Transmission (TOT) method using NIOSH 5040 protocol. A punch of quartz filter (1.5 cm × 1 cm) sample was taken and introduced into the OC/EC analyzer (Sunset Laboratory) with clean forceps. The organic compounds were vaporized and immediately oxidized to carbon dioxide in an oxidizer oven which follows the sample oven as the temperature (500 °C −700 °C) increased in four steps after purging with Helium gas. The flow of helium, containing the carbon dioxide, then goes to a methanator oven where the CO_2 is reduced to methane. The methane, then, is detected by a flame ionization detector (FID). The oven temperature increased to next level (850 °C) and all the elemental carbon content got oxidized and detected following the same process as for OC. Some portion of organic carbon (nearly 30%) can be converted to elemental carbon by pyrolytic conversion in the first step and hence it was continuously monitored by the laser beam transmitting through the filter to correct for this misclassification. Considering the FID response and laser transmission data overall OC and EC concentrations were calculated.

2.2. Quality control and quality assurance

During online sampling via AMS, important parameters (flow rate, filament current and voltages in mass spectrometer settings) of the instrument were regularly monitored and noted down on a daily basis. To verify mass accuracy, regular calibrations for calculating IE and RIE (relative ionization efficiency) of ammonium has been carried out before, during and after the campaign by atomizing pure NH_4NO_3 particles of 350 nm diameter into the AMS. In addition to that, pure $(NH_4)_2SO_4$ was also analyzed in the AMS, in order to determine different sulfate fragment ratios. Before entering into the AMS, ambient aerosols were dried using a silica gel drier (outlet RH < 20%) (Chakraborty et al., 2016a), to remove droplets and excess moisture/water, which can be detrimental to the AMS performance. Deviations in the IE values from successive calibrations were <5%; fewer variations were expected as no changes in AMS parameters or hardware have been made during the campaign. To characterize the influence of major gas phase species (like CO_2) on elemental ratios and AMS background signal on total mass, particle free air was sampled via AMS by placing a high efficiency particle attainment (HEPA) filter in front of AMS. The detection limit (DL) is calculated as 3*standard deviation of concentrations obtained from such particle free air sampling (Bahreini et al., 2003; DeCarlo et al., 2006; Drewnick et al., 2009; Salcedo et al., 2006). For different species, DL values are different with organics having highest DL value of 0.16 μg/m^3 and nitrate with minimum DL of 0.01 μg/m^3. AMS mass concentration measurement has an uncertainty of around 30% (Drewnick et al., 2008), while elemental ratios have an uncertainty of 7–12% (Aiken et al., 2008;

Canagaratna et al., 2015).

During offline ambient aerosol sampling, flow rate of the sampler was monitored at every 15 min interval during the 45 min sampling. After sampling, filters were always handled using powder free gloves and forceps, to further reduce the chance of contamination, before and after handling of filters, forceps were cleaned using Milli-Q water. Immediately after collection, filters were wrapped in aluminum foil and kept in sealed plastic pouches, which were then stored at −19 °C in the dark until further analysis. Field blanks were collected each day by placing a quartz filter inside the sampler for 45 min like actual sample filters but without drawing the air through it. Known amounts of reagent-grade crystalline sucrose and potassium hydrogen phthalate (KHP; 99.95%–100.05%), were analyzed to verify the OC fractions. To assure repeatability and precision, every sixth sample was examined in triplicates and analysis was rejected if variations were found to be >5%. After every 10 samples, instrument calibration was rechecked with known amount of sucrose. Detection limit for EC/OC analysis is taken as three times the standard deviation of field blank values. Average OC and EC values for field blanks are 0.21 ± 0.22 μg/cm^2 and 0.018 ± 0.036 μg/cm^2, respectively. Repeated analysis of blanks and standard samples revealed uncertainty values of 6% for OC and 8% for EC, respectively. All the reported offline values are blank corrected.

3. Results and discussions

3.1. Overall NR-PM$_1$ composition and characteristics

Campaign average NR-PM$_1$ loading is 40 μg/m^3, with the range varying from 9 to 144 μg/m^3. Daytime and nighttime average NR-PM$_1$ loadings are 35 and 45 μg/m^3, respectively (Fig. 2). Diurnal profiles (Fig. 3) of NR-PM$_1$ species concentration show significant changes throughout the day with lower values during mid-day and higher values during night time hours. The sampling site is located away from the industrial activities and most of the time wind blows the industrial plumes away from the sampling site (Rai et al., 2016). Traffic emission also reduced during mid afternoon after peaking in the morning rush hours. So observed decline in aerosol concentrations during afternoon is possibly due to a combination of reduced emissions, higher boundary layer heights and effective dispersion of pollutants.

Sulfate remained significantly higher compared to other species during mid-day, indicating its production via photochemical pathways. The overall NR-PM$_1$ composition is dominated by organics, contributing more than half (58%) to the total NR-PM$_1$ mass. Sulfate and Ammonium followed the organics with 25% and 10% contribution to total NR-PM$_1$ mass. Diurnal variation of NR-PM$_1$ composition (Fig. 3) revealed that during daytime contribution of sulfate became dominant, due to photochemical production and subsequent reduction in other species due to meteorology. Organic aerosols (OA) contributed more to NR-PM$_1$ during night, possibly due to enhanced primary emissions; like biomass burning, plying of heavy duty trucks within city limits (more details in section 3.1 for OA sources and composition) as reported in some previous studies (Kanawade et al., 2014; Ram et al., 2014). It is also possible that during daytime some relatively more volatile organics have escaped to the gas phase due to higher temperatures.

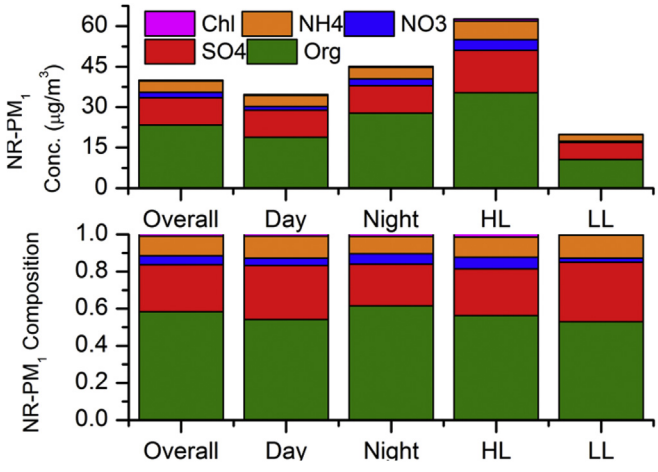

Fig. 2. NR-PM$_1$ concentrations and composition during different time periods of postmonsoon. HL, LL = High and low loading periods, respectively.

Aerosols were mostly neutral in nature; anions were neutralized by ammonium. ANR (aerosol neutralization ratio) was found to be 0.92.

$$\mathrm{ANR} = \frac{NH_4^+\ (m)}{18 \times \left(2 \times \frac{SO_4^{-2}\ (m)}{96} + \frac{NO_3^-\ (m)}{62} + \frac{Cl^-(m)}{35.5}\right)}$$

Where NH_4^+ (m), NO_3^-(m), SO_4^{-2}(m), and Cl^- (m) are mass concentrations of ammonium, nitrate, sulfate, and chloride, respectively (as measured by AMS). Although aerosols are neutralized, relatively higher NO^+/NO_2^+ ratios are observed (average = 5.5) for the campaign compared to the same ratio for pure NH_4NO_3 (= 2.8). The higher NO^+/NO_2^+ ratio in AMS generally indicates the presence of organo nitrates (ON) as they also produce NO^+ and NO_2^+ fragments which can't be distinguished from the same fragments produced by inorganic nitrates in AMS (Farmer et al., 2010). Observed NO^+/NO_2^+ ratio values (~3–20) in the campaign are also well within the range (~4–15) reported for different ON compounds and standards from previous AMS based studies (Bruns et al., 2010; Farmer et al., 2010; Fry et al., 2009). The presence of ON means that inorganic nitrates are possibly overestimated as some of the NO^+ and NO_2^+ fragments have actually originated from ON molecules. So, ANR values of aerosols are actually even higher, indicating complete neutralization. It is difficult to accurately calculate ON concentrations and contribution to total OA due to erroneous allocation of all NO^+ and NO_2^+ to inorganic nitrates and lack of ON standards analysis in this study. However, a lower bound of ON mass can be calculated based on the following approach described in Schurman et al. (2015).

$$\mathrm{ON_{min}} = (\mathrm{Org/OM{:}OC})^*(\mathrm{N{:}\ C})^*(14/12)$$

Calculations following this approach revealed that ON contributed at least 0.3 μg/m^3 or 1.1% to OA, with the range varying from 0.03 to 1.31 μg/m^3 and 0.3–6%, respectively. ON concentration values correlate well with BBOA and O-BBOA levels (R^2 = 0.36 & 0.58), indicating that most of ON may have originated from biomass burning activities. Lower night time NO^+/NO_2^+ ratios (average = 4.8) compared to daytime (average = 6.4), could be due to hydrolysis of ON groups due to higher night-time RH (Liu et al., 2012) and/or different nature of day and nighttime chemistry of ON molecules (Fry et al., 2013).

Key elemental ratios of OA revealed relatively higher O/C and OM/OC ratios (average = 0.66 and 1.99, respectively), indicating highly oxidized nature of OA. Observed OM/OC ratio is very close to the slope (= 2.1) obtained via plotting of AMS OM vs offline filter based OC concentrations (Fig. S1). Elemental ratios (Fig. 4a) also show strong diurnal variations with higher O/C and lowered H/C values during daytime due to photochemical oxidation and the lower influx of less oxidized primary OAs (POA). N/C ratios show the least variation in diurnal profile but slightly higher during early

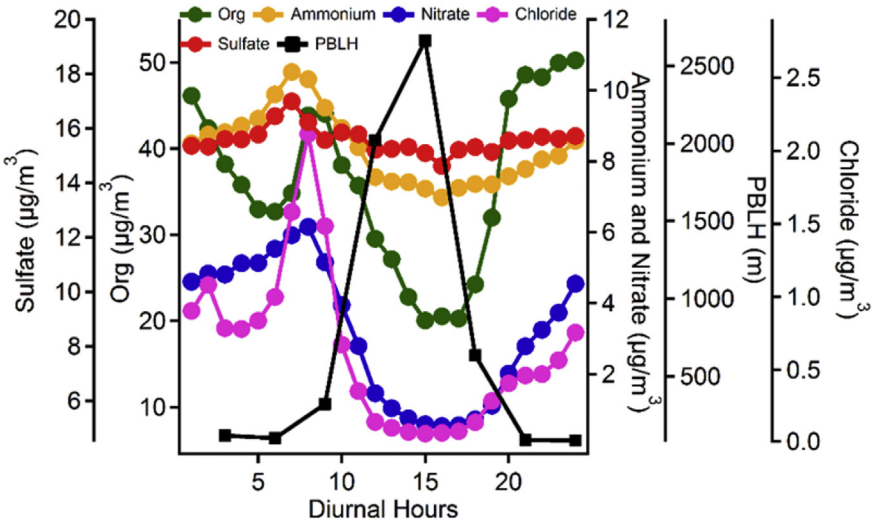

Fig. 3. Diurnal variations of different NR-PM_1 species and planetary boundary layer heights (PBLH). Diurnal variations are particularly prominent for some species (Organics, Nitrate, and Chloride) while relatively weak for other ones.

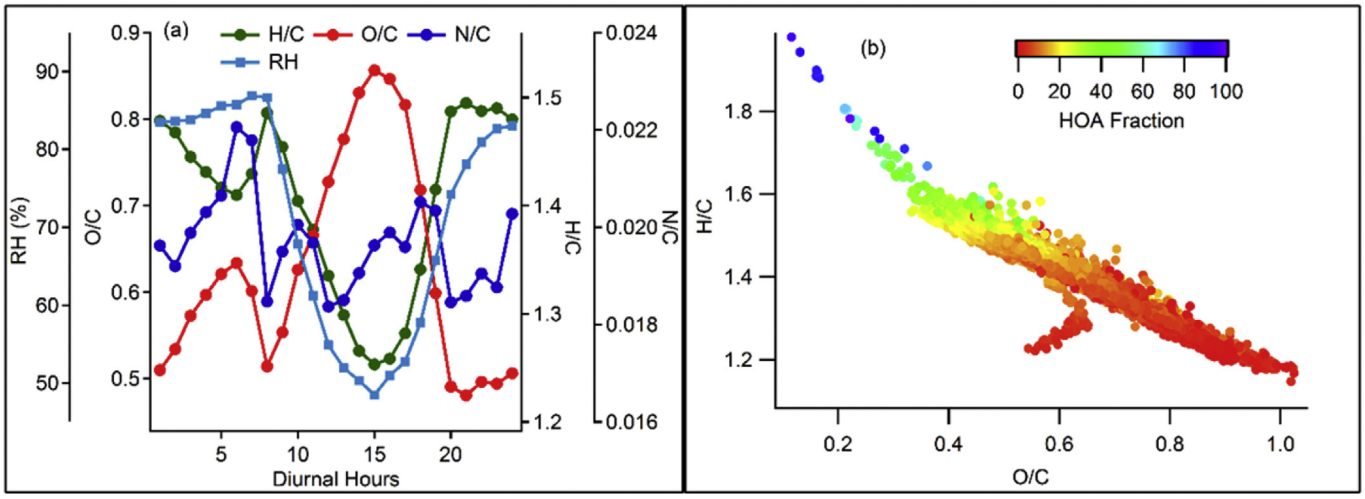

Fig. 4. a) Diurnal profiles of relative humidity (RH) and different elemental ratios of OA. b) Van Krevelen diagram is showing OA evolution and impact of primary OA on VK diagram slopes.

morning hours. Average night time O/C ratio (= 0.55) is much lower compared to daytime one (= 0.70) while the opposite is true for H/C ratios. A significant decrease in O/C ratios and enhancement in H/C ratios occur from evening to nighttime period. Most likely due to less efficient nocturnal processing, enhanced emissions and subsequent entrapment of primary OAs due to lower boundary layer. Van Krevelen (VK) (H/C vs O/C) diagram indicates that OA evolution has taken place along two different slopes; less oxidized organics (O/C ~ 0.05–0.35) have evolved along a very steep slope, and relatively more oxidized ones followed a much milder slope (Fig. 4b). During the initial phase of oxidation, even an addition of small amount oxygenated moieties to the non/less oxidized organic molecule can cause a steep decline in H/C ratios. As oxidation progresses, the addition of oxygenated moieties has less impact on elemental ratios, resulting in a milder slope. It is also possible that at later stages of oxidation, fragmentation of already oxidized OA (Kroll et al., 2009) is taking place leading to a shallower slope. Diurnal O/C ratios show steep decrease around 9–10 a.m. and 6–8 p.m. with subsequent enhancement in H/C ratios, traffic related less oxidized POA emissions are responsible for such changes. Day and night time VK diagram slopes are very similar, however, a part of OA (very less oxidized) which evolved along a much steeper slope as mentioned earlier, present only during night time.

3.2. OA sources and composition

Based on source apportionment using PMF (Lanz et al., 2007; Ulbrich et al., 2009) on organics mass spectra of AMS, 6 factor solution was chosen (Fig. 5). These factors were chosen based on their mass spectra, elemental ratios, diurnal pattern, comparison with reference mass spectra –(http://cires.colorado.edu/jimenez-group/AMSsd) and correlation with external tracers. Brief details on PMF model and rationales of choosing 6 factors, PMF diagnostics and comparison with reference mass spectra (Figs. S2 and S3) are given in supplementary section (section S1). Among 6 factors are different types of oxidized/secondary OA (OOA), including one secondary biomass burning OA (O-BBOA) and primary OAs like BBOA, Hydrocarbon like OA (HOA). Among different types of oxidized OAs, two relatively less oxidized, semi-volatile OOAs (SVOOA-1,2) were identified with very similar mass spectra and

elemental ratios. It is possible that they have formed via atmospheric processing of similar types of precursor organics at a similar or different time scale. So, time series of those two factors are combined as one factor (SVOOA), this has also been done in many previous studies (Chakraborty et al., 2016c; Schurman et al., 2015) and also suggested by Ulbrich et al. (2009).

The first factor is the most oxidized among all other factors with an O/C ratio of 1.12, and an f44/f43 ratio of 5.43. In AMS data, f44 (m/z 44/OA) is considered to be the marker for more oxidized, less volatile organic acids. Similarly, f43 (m/z 43/OA) is considered to be the marker for more volatile and less oxidized carbonyl moieties (Ng et al., 2011; Takegawa et al., 2009, 2005). Higher f44 level indicates that OA is mostly composed of highly oxidized organic acids, and the higher f44/f43 ratio also suggests that it's relatively less volatile in nature. So, this factor is termed as low volatile OOA or LVOOA, this factor also has a good correlation with inorganic sulfate (Fig. S4), pointing towards its aged and low volatile nature. Diurnal profile (Fig. 6) of LVOOA peaks around afternoon in spite of boundary layer expansion and dilution, while all other factors show a steep decline. This trend clearly indicates that during the daytime, intense photochemical activities are responsible for LVOOA production. Back trajectory analysis indicates that LVOOA received significant contributions from transported aerosols (Fig. S5), in line with its highly oxidized/processed nature. Very high fraction of this factor also seems to be coming from ocean, indicating possible marine biogenic secondary OA contribution to LVOOA. Secondary OA from marine biogenic precursors can be highly oxidized (Anttila et al., 2010; Bikkina et al., 2014) and may have contributed to very high O/C of this factor.

The second factor is identified as Oxidized/secondary BBOA (O-BBOA) as it contains a significant fraction of $C_2H_4O_2^+$ fragment (a marker for biomass burning in AMS, originates from the fragmentation of Levoglucosan; Aiken et al., 2010, Cubison et al., 2011) and also has a much higher O/C ratio (= 0.79) compared to the primary

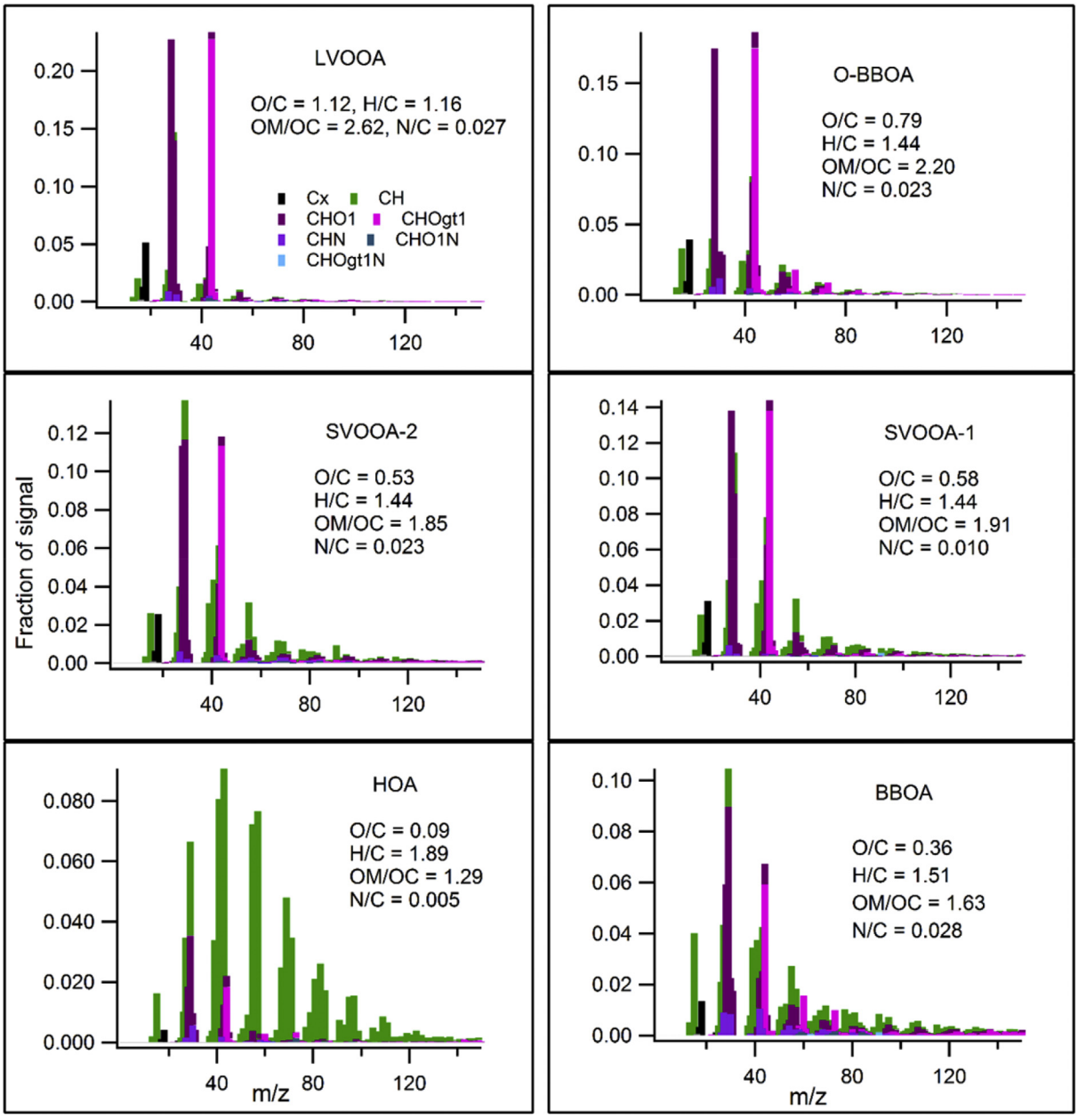

Fig. 5. Six-factor PMF solution with several types of secondary and primary OA factors.

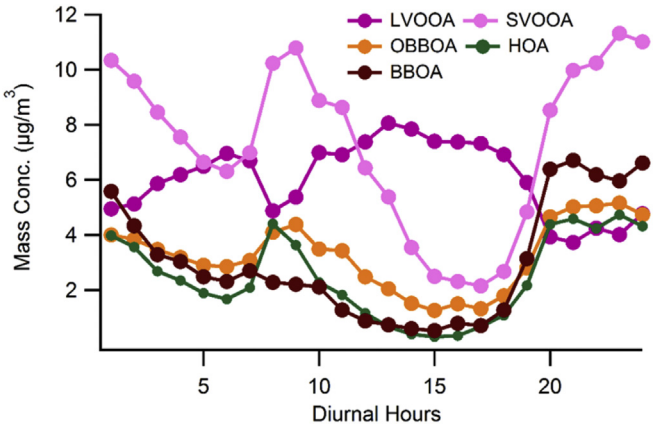

Fig. 6. Diurnal variations of different types of OA. Primary and less oxidized OOAs are dominating during the night while LVOOA dominates during the daytime.

BBOA. Its contribution to total OA is also higher than primary BBOA. Interestingly, though O-BBOA is much more oxidized compared to SVOOAs, it still has similar H/C ratio as SVOOAs. Generally, H/C and O/C ratios follow an opposite trend but retaining higher H/C ratio even at very high O/C ratio indicate that it has possibly evolved from oxidation/processing of primary BBOA. Similar characteristics of O-BBOA were reported from the same location during winter of 2012–13 (Chakraborty et al., 2015). It's diurnal variation (Fig. 6) is slightly different from primary BBOA, with a higher afternoon concentration than primary OAs. However, during night time its enhancement is much lesser than primary BBOA, possibly due to less efficient oxidation/processing. O-BBOA has good correlation with m/z 60 (m/z associated with biomass burning sources) and moderate correlation with sulfate, another indication that this secondary BBOA is possibly a product of primary OA oxidation/processing. Back trajectory analysis indicates (Fig. S5) that O-BBOA is mostly confined to nearby areas, as also observed in a previous study (Chakraborty et al., 2015) from this location. Most likely O-BBOA is locally formed through photochemical oxidation of primary BBOA.

SVOOA -1 and 2 (semi-volatile OOA; SVOOA-1+SVOOA-2), both have much lower O/C ratios than LVOOA but higher than other primary OAs (HOA, BBOA). They also have lower f44/f43 ratios (= 2.8 & 2.3 for SVOOA-1 & 2, respectively) compared to LVOOA, suggesting their semi-volatile nature. Overall, SVOOAs (SVOOA-1+SVOOA-2) contributed most to the total OA and also have a moderately good correlation with inorganic nitrate (Fig. S4), hinting towards their freshly oxidized and semi-volatile nature. The diurnal trend of SVOOA mass concentration (Fig. 6) shows that it reaches a peak level soon after the morning traffic rush hours or HOA peak. This may be an indication that SVOOA is forming via oxidation of freshly emitted POAs. Later in the day, SVOOA concentration follows a declining trend possibly due to boundary layer expansion and its conversion to more oxidized LVOOA. Back trajectory analysis indicates that both types of SVOOA received contributions from both regional and long range transported aerosols. However, SVOOA-1 seems to be mostly transported via aerosols from North-Western India where a lot of primary OAs are being generated due to the burning of paddy residues. This again hints towards formation of SVOOA via oxidation of primary OAs.

HOA or hydrocarbon like OA has the lowest O/C (= 0.09), and highest H/C (= 1.89) ratio among all the factors and the ratios are well within the range (0.06–0.18) reported for HOA factor worldwide (Aiken et al., 2008; Canagaratna et al., 2015). Several hydrocarbon fragments clearly dominate its mass spectra. It's diurnal variation also peaked during morning traffic rush hours and decreased steeply during the afternoon due to reduced traffic emissions, possible conversion to OOAs and boundary layer expansion. Night time enhancements (Fig. 6) in HOA concentration are probably due to lowering of boundary layer and emissions from heavy duty vehicles plying within the city from late evening (after 9 p.m.). HOA has the lowest contribution among other factors, indicating that by the time aerosol reached the measuring site, they were mostly processed. Back trajectory analysis also indicates that HOA mostly arrived at the measurement sites from nearby states and possibly processed to secondary OA during transport.

Primary BBOA or BBOA factor is identified based on characteristics signal at m/z 60 ($C_2H_4O_2^+$) & 73 ($C_3H_5O_2^+$). It has a moderate O/C ratio, as OA emitted from biomass burning itself contain some amount of oxidized fragments. Observed O/C ratio is well within the typical range reported for BBOA from studies around the world (Aiken et al., 2010; Cubison et al., 2011). Its diurnal pattern shows that it's mostly dominating during night time when most of the local burning activities take place. As the afternoon approaches, BBOA concentration goes down steeply possibly due to dilution by higher boundary layer and/or conversion to O-BBOA. It has the second lowest contribution to total OA after HOA, which is expected as local biomass burning activities peak from November at the onset of winter. Back trajectory analysis also shows that transported aerosols from Northern and Western India also contributed significantly to the observed BBOA levels. This is in line with post monsoon paddy residue burning activities in Northern and Western states of India.

Overall, OOAs (SVOOA + LVOOA + O-BBOA) dominate OA composition, contributing 75% of the total OA. This dominance is even more pronounced during daytime when 84% of total OA are OOAs (Fig. 7). This observation of the dominance of OOAs during daytime is also supported by very high OC/EC ratios of daytime (average = 8.10), clearly indicating significant contributions from secondary OC components. OOAs dominate nighttime OA as well but to a lesser extent, which is expected because of no photochemical activities and accumulation of primary OA emissions due to lower boundary layer and higher atmospheric stability. During daytime, LVOOA is the dominating OOA, clearly showing the impact of highly oxidized secondary OA formations via photochemistry. Nighttime higher SVOOA could be due to enhanced gas to particle partitioning of less oxidized gas phase products because of higher loading and lower temperatures. It's also possible that less efficient nocturnal chemical processing (like aqueous phase oxidation) also

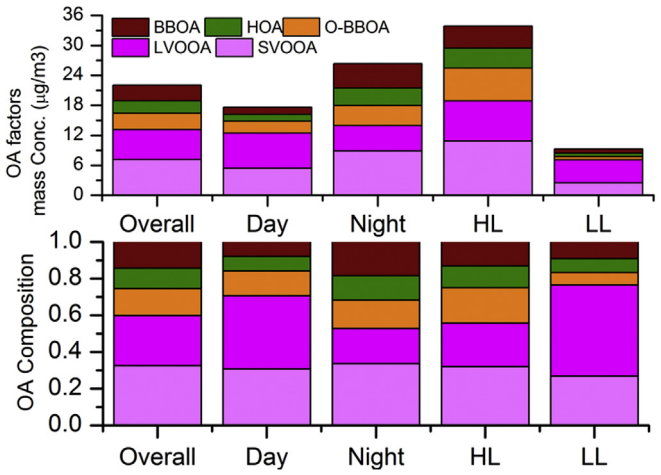

Fig. 7. OA concentrations and composition during different time periods of post monsoon. HL, LL = High and low loading periods, respectively.

contributed to OOAs (Chakraborty et al., 2016a, 2015).

3.3. High and low loading events

To evaluate the differences in OA composition, characteristics, and chemistry in different loading conditions, the whole campaign is further divided into high (HLE) and low loading events (LLE). HLE and LLE events are an agglomeration of time periods with overall NR-PM_1 loading > 75th percentile (> 51 μg/m^3 and < 25th percentile (< 26 μg/m^3) of the campaign NR-PM_1 mass concentration values, respectively. Average NR-PM_1 loading values for HLE and LLE events are 63 μg/m^3 and 20 μg/m^3, respectively (Fig. 2) and much different from campaign average NR-PM_1 loading of 40 μg/m^3. Chloride and Nitrate show maximum relative change from HLE to LLE with 10 and 9 fold decreases in their concentration, respectively. In terms of absolute values, decrease in OA was largest with a reduction of 25 μg/m^3 mass concentration from HLE to LLE. However, for HLE and LLE, OA remain the dominant specie, followed by sulfate as the overall campaign average composition. Sulfate contributions to NR-PM_1 are much higher during LLE compared to HLE. LL events are mostly associated with daytime hours (~70% of total LLE periods), so enhanced photochemistry possibly caused higher sulfate production. Nitrate/sulfate ratios are much higher during HLE (average = 0.25) than LLE (average = 0.07), showing higher dominance of vehicular emissions in HLE than LLE. This is also supported by OA composition as discussed later in this section. The impact of primary emissions is generally reduced during daytime due to less active local emission sources and dilution due to elevated boundary layer. Reduced levels of primary pollutants may have also enhanced the efficiency of primary pollutants processing and production of secondary species (like sulfate, secondary OA).

Apart from OA mass concentrations, the composition also shows drastic changes from HLE to LLE periods (Fig. 7). Total OOA (SVOOA + LVOOA + O-BBOA) contribution to OA increased from 75% to 84% from HLE to LLE, while the dominant t OOA type changed from SV-OOA to LVOOA (Fig. 6). LVOOA shows the most drastic change, as its contribution to total OA almost halved to 27% during HLE from 52% of LLE. All primary OAs (HOA & BBOA) along with O-BBOA show a steep increase (5–10 times) from LLE to HLE (Fig. 7), clearly indicating more primary OA emissions. Most of HLE time periods (~75%) being associated with nighttime hours, so relatively higher emissions, lower boundary layer and less secondary production due to the absence of photochemistry, may have caused such enhancements. During LLE, the dominance of LVOOA is more pronounced than the dominance of SVOOA during HLE. Higher OA loading enhanced the partitioning of less oxidized gas phase oxidation products leading to the dominance of less oxidized semi volatile organics. On the contrary, under lower OA loading condition more oxidized and less volatile organics partitioned into the particle phase. The absolute and relative increase in SVOOA concentration and contributions from LLE to HLE (Fig. 7) supports the loading dependent partitioning of oxidized OAs. Overall, O/C ratio (= 0.59) during HLE is significantly lower than the average O/C ratio (= 0.76) of LLE, further showing the dominance of less oxidized organics during HLE.

Even when only daytime hours of HLE and LLE are considered, OA composition during LLE is more dominated by LVOOA (48% vs 30%) and has a much higher O/C ratio of 0.79 compared to 0.63 of HLE. Similarly, night time OOA from LLE is more oxidized (O/C = 0.64) than the OOA from HLE nights (O/C = 0.57). The difference between average night time O/C ratios of HLE and LLE (= 0.07) is much lower than the same between daytime average O/C ratios (= 0.16). This is possibly due to more efficient oxidation of gas phase precursor organics during daytime via photochemistry and subsequent partitioning of those highly oxidized products. During this partitioning, OA loading played a vital role (causing enhanced partitioning of highly oxidized organics during LLE) and widened the differences between HLE and LLE O/C ratios. Another possibility is that during HLE, emissions of primary OAs were higher, which caused this lower O/C ratio compared to LLE periods. However, with an increase in OA loading fractional contribution of $C_2H_3O^+$ fragment (m/z 43), which is often considered as the marker of less oxidized and semi-volatile organics (like Aldehydes, Ketones etc.) (Ng et al., 2011; Takegawa et al., 2006b) also increases (Fig. S6). This indicates that contribution of semi-volatile organics is increasing with OA loading, signaling enhanced partitioning of semi-volatile organics. On the contrary, with an increase in OA loading fractional contribution of CO_2^+ fragment (m/z 44), which is often considered as the marker of more oxidized and less volatile organics (like organic acids and peroxides) (Ng et al., 2011; Takegawa et al., 2006a) decreases rapidly (Fig. S6). Laboratory studies (Kang et al., 2011; Pfaffenberger et al., 2013; Shilling et al., 2009) have also reported similar behavior of fCO_2^+ and $fC_2H_3O^+$ from low to high loading transitions during oxidation of known organic precursors. This phenomenon is attributed to the preferential partitioning of less oxidized organics from gas to particle phase at higher OA loadings. Similar observations in this study along with the dominance of POAs at higher loadings indicate that lower O/C ratios during HLE were most likely caused by a combination of enhanced primary OA emission coupled with enhanced partitioning of less oxidized organics to particulate phase.

3.4. Comparison of post monsoon OA composition and chemistry with monsoon and winter period

During 2014-15, real-time aerosol sampling was also carried out during monsoon (Chakraborty et al., 2016c) and winter season (Chakraborty et al., 2016b). This allowed us to look into the evolution of OA composition and chemistry from monsoon to winter for the first time under very complex environmental conditions of IGP. For more details on Monsoon and winter time OA characteristics of 2014–15 period, please look into Chakraborty et al. (2016b, 2016c). NR-PM_1 (Fig. 8) loading varied significantly among these 3 seasons with wintertime loading being highest and lowest during monsoon. This is mainly due to a combination of meteorological factors and emission characteristics. During winter, local/regional biomass burning emissions are much higher and atmospheric conditions are quite stable (with lower temperature, wind speed, and boundary layer height) than monsoon or post monsoon, thus effectively trapping all pollutants. During monsoon, frequent washout by rainfall along with more favorable meteorological conditions (high wind speed, temperature, and higher boundary layer) for pollutant dispersion caused lower loadings than winter or post monsoon.

During post monsoon season, long-range transported organic aerosols emitted from paddy residue burnings in North-Western India (Punjab-Haryana) (Chakraborty et al., 2015; Rajput et al., 2011; Rastogi et al., 2014) generally leads to more aerosol loadings in IGP region. However, the overall composition of NR-PM_1 is completely dominated by organics during all 3 seasons (Fig. 8), indicating presence of active OA sources and formation of secondary OA throughout the year irrespective of loading or atmospheric conditions. During winter, nitrate was the second most dominant species after organics while for other two seasons, it is sulfate. Lower temperatures, higher humidity and enhanced NOx emissions (Gaur et al., 2014) possibly caused this higher nitrate fraction during winter, while relatively less SOx emissions (Gaur et al., 2014) coupled with weak solar radiation may have hampered sulfate production.

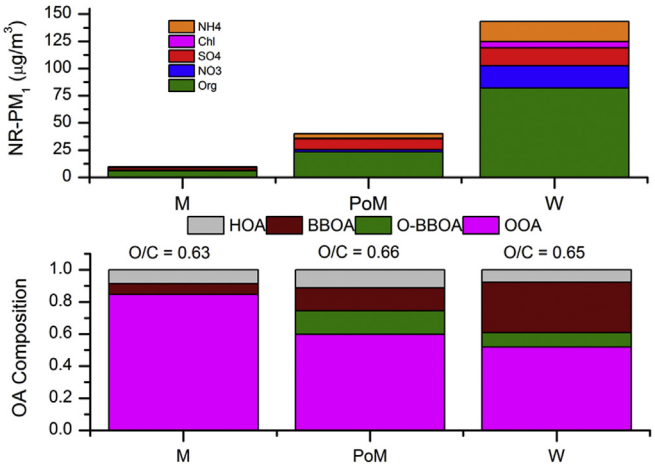

Fig. 8. NR-PM_1 composition and concentration in different seasons. For all seasons OOA = sum of different types of OOAs (LV or SVOOAs). M = Monsoon, PoM = Post monsoon, W = Winter.

Although overall NR-PM_1 compositions are dominated by OA for all seasons, a closer look into OA composition and chemistry reveal significant differences from one season to another. All 3 seasons are dominated by secondary/oxidized OA but that dominance was most pronounced during monsoon season than post monsoon or winter (Fig. 8). As mentioned earlier, during post monsoon and winter, local and regional biomass burning activities are much more prominent than monsoon. Higher emissions coupled with more cooler and stable environment enhance the primary BBOA contributions. Another interesting difference is the presence of a secondary/oxidized BBOA (O-BBOA) during post monsoon and winter. This indicates that BBOA emitted from enhanced burning activities are being oxidized either during transport or locally. A previous winter study from this location (Chakraborty et al., 2015) indicated that most of this O-BBOA were actually restricted to nearby areas of the sampling. Stagnant conditions and enhanced aqueous chemistry due to fog and elevated RH levels may have created a suitable environment for primary BBOA processing, as observed in polluted and fog affected region of Po Valley (Gilardoni et al., 2016).

However, overall O/C ratios from 3 different seasons are relatively higher and rather similar in spite of significant variations in OA composition and loadings. This is a bit surprising as higher OA loadings usually lead to lower O/C ratios. This apparent discrepancy can be explained in terms of seasonal differences in meteorological conditions, emission characteristics and ambient processing of OA. For example, lower temperatures in winter make it easier for oxidized organics from gas phase to partition into phase and remain there. High RH and frequent fog events can produce highly oxidized OA via aqueous processing irrespective of OA loading conditions (Chakraborty et al., 2016a, 2016b; Ervens et al., 2011). In monsoon, days are mostly cloudy with frequent rain events. Lower photochemistry along with the possible efficient removal of oxidized OA via rain may have prevented very high O/C ratios under very low loading conditions of monsoon period. Similar O/C ratios also indicate that during post monsoon and winter although total OOA contribution is lower but identified OOAs are more oxidized than in monsoon. Indeed, mass spectra and elemental ratios of identified OOAs varied significantly from one season to another. During winter, O/C ratios of different types of identified OOAs varied from 0.7 to 1.2, while the ranges during monsoon and post monsoon were 0.4–1.2 and 0.5–1.1, respectively. This indicates that most highly oxidized and low volatile OAs have similar elemental ratios throughout the year as maximum O/C ratios have a very narrow range (from 1.1 to 1.2). On the contrary, the relatively less oxidized/semi volatile OOAs have a broad range of O/C ratios (0.4–0.7), varying significantly from one season to another. O-BBOA mass spectra and O/C ratios are also very similar during winter and post monsoon. Interestingly, variations in HOA mass spectra and corresponding elemental ratios were minimal compared to all other types of OA. O/C ratios of HOA from monsoon to winter lie within a very narrow range of 0.05–0.09, indicating that their nature varies little with season or meteorology. This is not unexpected as nature of vehicular/industrial emission sources (from which HOA generally originates; Zhang et al., 2007, 2005) hardly changes from one season to another. Mass spectra and elemental ratios of primary BBOAs are also not very different during monsoon (O/C = 0.36) and post-monsoon (O/C = 0.45). However, during winter, several types of BBOAs have been identified in previous studies (Bhattu and Tripathi, 2015; Chakraborty et al., 2016b, 2015). During monsoon and post monsoon, local biomass burning activities are much lower than winter and BBOAs generally comes from regional burning activities (like paddy residue burnings in North-Western India). During winter, local biomass burning activities increased many folds (Kaul et al., 2011; Tripathi et al., 2006) as local people burn different types of biomass (leaves, trash, wood, cow dung, plastic, tires, etc.) to get respite from cold. Therefore, the presence of several types of BBOAs with different mass spectra and elemental ratios are not surprising.

Although in terms of overall O/C ratios, 3 seasons are not very different, but the diurnal pattern of O/C ratios (Fig. 9) indicate some subtle differences. Night time O/C ratios are generally higher during monsoon and winter compared to post monsoon, whereas daytime O/C ratio is highest during post monsoon. This results in higher day and nighttime O/C ratio difference in post monsoon than other 2 seasons. During monsoon and winter, night time RH is much higher than post monsoon one which may have resulted in the significant amount of aqueous processing. Especially during winter, persistent fog and haze episodes during night time may have contributed to enhanced night time OA processing as shown in previous studies from this location (Chakraborty et al., 2016a, 2016b, 2015). Rain and fog water characteristics from monsoon and winter season (Chakraborty et al., 2016a, 2016c) also showed several signs (much higher O/C ratios than background OA, the presence of organosulfur fragments) of significant aqueous phase processing. Despite rain and fog scavenging of OA (especially of OOAs due to their higher O/C ratios and polarity) (Gilardoni et al., 2014), O/C ratios of monsoon and winter periods were similar or higher than post monsoon. This indicates that removal of OOAs by fog/rain may have been offset by production of highly oxidized OOA (possibly in aqueous phase). Daytime solar radiation during winter and monsoon are relatively

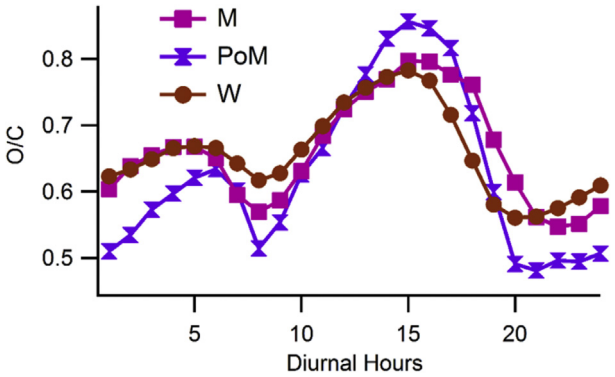

Fig. 9. Diurnal O/C ratios for different seasons showing some subtle differences in OA evolution throughout the day.

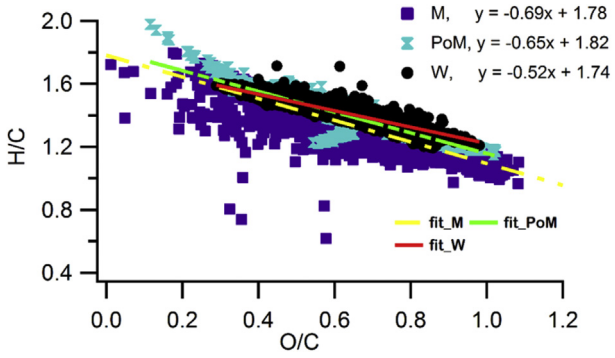

Fig. 10. Van Krevelen diagram (H/C vs O/C) for different seasons, showing changes in slope (due to changes in chemistry and/or composition) through which OA evolves during different seasons of the year.

weaker than post monsoon due to persistent foggy/hazy (for winter) and cloudy (for monsoon) conditions. This may have caused the lowering of peak daytime O/C ratios during monsoon and winter as compared to post-monsoon (Fig. 9).

Van Krevelen (VK) diagram (Fig. 10) also highlights some differences in OA evolution among 3 seasons. From monsoon to winter, slopes of VK diagram has become shallower, which means that increase in O/C ratio during winter associated with a less steep decrease in H/C ratios as compared to other 2 seasons. Shallower slope of ~0.5 in VK diagram generally indicates the addition of carboxylic and/or hydroxyl group to the carbon backbone of an organic molecule and subsequent fragmentation of that carbon backbone (Heald et al., 2010; Ng et al., 2011). While steeper slope generally indicates the addition of carbonyl moieties without fragmentation or a functionalization process (Heald et al., 2010; Ng et al., 2011). This suggests that mechanism of OA oxidation may have varied from one season to other. Another interesting observation of VK diagram is that for similar O/C ratios, winter and post monsoon tend to have higher H/C ratios (Fig. 10). This is actually caused by the presence of O-BBOA during post monsoon and winter as it has higher O/C ratio and similar or higher H/C ratios compared to other less oxidized OOAs (like SV-OOA in Fig. 5). Triangle plot (f44 vs f43, Fig. 11) also reveals some differences in OA mass spectra from 3 seasons in spite of having similar O/C ratios. The dominance of highly oxidized organic acids (carboxylic acids, indicated by f44 levels in AMS) is more pronounced during monsoon than winter or post monsoon, while during winter less oxidized aldehyde/ketone fragments also contributed more significantly than in other two seasons.

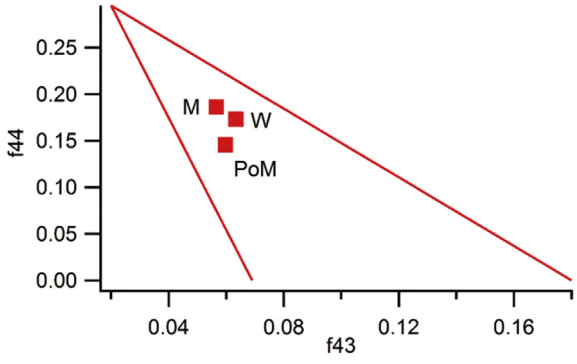

Fig. 11. Triangle plot showing the average position of overall OA of different seasons in f44 (m/z 44/OA) vs f43 (m/z 43/OA) space.

4. Conclusions

Real-time submicron aerosol characterization during post monsoon season revealed the dominance of OA in aerosol composition. Aerosols were found to be completely neutralized, and the presence of organo nitrates has been detected. Organic aerosols were found to be significantly oxidized and dominated by oxidized OAs as revealed via source apportionment. The negative impact of higher OA loading is clearly visible on OA composition and oxidation ratios with higher OA loading leading to lower O/C ratios. This is due to a combination of POA dominance at higher OA loading and enhanced gas to particle partitioning of less oxidized gas phase organics. The presence of a secondary BBOA indicate atmospheric processing of emitted primary BBOAs during transport and/or due to local processing. A comparison with other seasons revealed some interesting differences in terms of OA composition and chemistry. During winter and post monsoon season OA has evolved along shallower slopes than monsoon season, highlighting differences in chemistry and/or OA sources. In spite of very high OA loading, winter time OA was found to be equally oxidized as monsoon and post monsoon. This observation is possibly a result of enhanced aqueous chemistry and stagnant condition during wintertime which allowed more effective processing of OA. BBOAs of both primary and secondary nature are far more dominant during winter and post monsoon than monsoon season due to enhanced local and regional biomass burning activities. Similar overall O/C ratios in spite of very different OOA contributions revealed that nature of OOAs (especially of SVOOAs) and possibly their formation mechanisms vary significantly from one season to another. The dominance of secondary/oxidized OAs in all seasons indicate that an effective control strategy should take into account the strength of local/regional primary sources and oxygenation capacity of the environment to produce secondary OA from those primary emissions.

Acknowledgements

Authors acknowledge partial funds received from Indian National Science Academy to carry out this study. HR-TOF-AMS was acquired via a generous one-time grant from IIT Kanpur. S.N.Tripathi also acknowledges the financial support received from the Department of Biotechnology (India).

Appendix A. Supplementary data

Supplementary data related to this article can be found at https://doi.org/10.1016/j.envpol.2017.09.079.

References

Aiken, A.C., de Foy, B., Wiedinmyer, C., DeCarlo, P.F., Ulbrich, I.M., Wehrli, M.N., Szidat, S., Prévôt, A.S.H., Noda, J., Wacker, L., Volkamer, R., Fortner, E., Wang, J., Laskin, A., Shutthanandan, V., Zheng, J., Zhang, R., Paredes-Miranda, G., Arnott, W.P., Molina, L.T., Sosa, G., Querol, X., Jimenez, J.L., 2010. Mexico city aerosol analysis during MILAGRO using high resolution aerosol mass spectrometry at the urban supersite (T0) - Part 2: analysis of the biomass burning contribution and the non-fossil carbon fraction. Atmos. Chem. Phys. 10, 5315–5341. https://doi.org/10.5194/acp-10-5315-2010.

Aiken, A.C., Decarlo, P.F., Kroll, J.H., Worsnop, D.R., Huffman, J.A., Docherty, K.S., Ulbrich, I.M., Mohr, C., Kimmel, J.R., Sueper, D., Sun, Y., Zhang, Q., Trimborn, A., Northway, M., Ziemann, P.J., Canagaratna, M.R., Onasch, T.B., Alfarra, M.R., Prévôt, A.S.H., Dommen, J., Duplissy, J., Metzger, A., Baltensperger, U., Jimenez, J.L., 2008. O/C and OM/OC ratios of primary, secondary, and ambient organic aerosols with high-resolution time-of-flight aerosol mass spectrometry. Environ. Sci. Technol. 42, 4478–4485. https://doi.org/10.1021/es703009q.

Anttila, T., Langmann, B., Varghese, S., O'Dowd, C., 2010. Contribution of isoprene oxidation products to marine aerosol over the North-East Atlantic. Adv. Meteorol. 2010, 1–10. https://doi.org/10.1155/2010/482603.

Bahreini, R., Jimenez, J.L., Wang, J., Flagan, R.C., Seinfeld, J.H., Jayne, J.T.,

Worsnop, D.R., 2003. Aircraft-based aerosol size and composition measurements during ACE-Asia using an Aerodyne aerosol mass spectrometer. J. Geophys. Res. 108 https://doi.org/10.1029/2002jd003226.
Bhattu, D., Tripathi, S.N., 2015. CCN closure study: effects of aerosol chemical composition and mixing state. J. Geophys. Res. Atmos. 120, 766–783. https://doi.org/10.1002/2014JD021978.
Bikkina, S., Kawamura, K., Miyazaki, Y., Fu, P., 2014. High abundances of oxalic, azelaic, and glyoxylic acids and methylglyoxal in the open ocean with high biological activity: implication for secondary OA formation from isoprene. Geophys. Res. Lett. 41, 3649–3657. https://doi.org/10.1002/2014GL059913.
Bruns, E.A., Perraud, V., Zelenyuk, A., Ezell, M.J., Johnson, S.N., Yu, Y., Imre, D., Finlayson-Pitts, B.J., Alexander, M.L., 2010. Comparison of FTIR and particle mass spectrometry for the measurement of particulate organic nitrates. Environ. Sci. Technol. 44, 1056–1061. https://doi.org/10.1021/es9029864.
Canagaratna, M.R., Jayne, J.T., Jimenez, J.L., Allan, J.D., Alfarra, M.R., Zhang, Q., Onasch, T.B., Drewnick, F., Coe, H., Middlebrook, A., Delia, A., Williams, L.R., Trimborn, A.M., Northway, M.J., DeCarlo, P.F., Kolb, C.E., Davidovits, P., Worsnop, D.R., 2007. Chemical and microphysical characterization of ambient aerosols with the aerodyne aerosol mass spectrometer. Mass Spectrom. Rev. 26, 185–222. https://doi.org/10.1002/mas.20115.
Canagaratna, M.R., Jimenez, J.L., Kroll, J.H., Chen, Q., Kessler, S.H., Massoli, P., Hildebrandt Ruiz, L., Fortner, E., Williams, L.R., Wilson, K.R., Surratt, J.D., Donahue, N.M., Jayne, J.T., Worsnop, D.R., 2015. Elemental ratio measurements of organic compounds using aerosol mass spectrometry: characterization, improved calibration, and implications. Atmos. Chem. Phys. 15, 253–272. https://doi.org/10.5194/acp-15-253-2015.
Chakraborty, A., Bhattu, D., Gupta, T., Tripathi, S.N., Canagaratna, M.R., 2015. Real-time measurements of ambient aerosols in a polluted Indian city: sources, characteristics and processing of organic aerosols during foggy and non-foggy periods. J. Geophys. Res. Atmos. 120, 9006–9019. https://doi.org/10.1002/2015JD023419.
Chakraborty, A., Ervens, B., Gupta, T., Tripathi, S.N., 2016a. Characterization of organic residues of size-resolved fog droplets and their atmospheric implications. J. Geophys. Res. Atmos. 121, 4317–4332. https://doi.org/10.1002/2015JD024508.
Chakraborty, A., Gupta, T., 2010. Chemical characterization and source apportionment of submicron (PM1) aerosol in Kanpur region, India. Aerosol Air Qual. Res. 10, 433–445. https://doi.org/10.4209/aaqr.2009.11.0071.
Chakraborty, A., Gupta, T., Tripathi, S.N., 2016b. Combined effects of organic aerosol loading and fog processing on organic aerosols oxidation, composition, and evolution. Sci. Total Environ. 573, 690–698. https://doi.org/10.1016/j.scitotenv.2016.08.156.
Chakraborty, A., Gupta, T., Tripathi, S.N., 2016c. Chemical composition and characteristics of ambient aerosols and rainwater residues during Indian summer monsoon: insight from aerosol mass spectrometry. Atmos. Environ. 136, 144–155. https://doi.org/10.1016/j.atmosenv.2016.04.024.
Cubison, M.J., Ortega, A.M., Hayes, P.L., Farmer, D.K., Day, D., Lechner, M.J., Brune, W.H., Apel, E., Diskin, G.S., Fisher, J.A., Fuelberg, H.E., Hecobian, A., Knapp, D.J., Mikoviny, T., Riemer, D., Sachse, G.W., Sessions, W., Weber, R.J., Weinheimer, A.J., Wisthaler, A., Jimenez, J.L., 2011. Effects of aging on organic aerosol from open biomass burning smoke in aircraft and laboratory studies. Atmos. Chem. Phys. 11, 12049–12064. https://doi.org/10.5194/acp-11-12049-2011.
DeCarlo, P.F., Kimmel, J.R., Trimborn, A., Northway, M.J., Jayne, J.T., Aiken, A.C., Gonin, M., Fuhrer, K., Horvath, T., Docherty, K.S., Worsnop, D.R., Jimenez, J.L., 2006. Field-deployable, high-resolution, time-of-flight aerosol mass spectrometer. Anal. Chem. 78, 8281–8289. https://doi.org/10.1021/ac061249n.
Draxler, R., Rolph, G.D., 2003. HYSPLIT (Hybrid Single-particle Lagrangian Integrated Trajectory) Model Access via NOAA ARL READY Website. NOAA air resources laboratory, Silver spring, MD USA. NOAA. http://www.arl.noaa.gov/ready/hysplit4.html.
Draxler, R., Stunder, B., Rolph, G., Stein, A., Taylor, A., 2014. HYSPLIT4 User 's Guide. NOAA.
Drewnick, F., Hings, S.S., Alfarra, M.R., Prevot, A.S.H., Borrmann, S., 2009. Aerosol quantification with the Aerodyne Aerosol Mass Spectrometer: detection limits and ionizer background effects. Atmos. Meas. Tech. 2, 33–46.
Drewnick, F., Hings, S.S., Alfarra, M.R., Prévôt, A.S.H., Borrmann, S., 2008. Aerosol quantification with the Aerodyne Aerosol Mass Spectrometer: detection limits and ionizer background effects. Atmos. Meas. Tech. Discuss. 1, 169–204.
Drewnick, F., Hings, S.S., DeCarlo, P., Jayne, J.T., Gonin, M., Fuhrer, K., Weimer, S., Jimenez, J.L., Demerjian, K.L., Borrmann, S., Worsnop, D.R., 2005. A new time-of-flight aerosol mass spectrometer (TOF-AMS)—instrument description and first field deployment. Aerosol Sci. Technol. 39, 637–658. https://doi.org/10.1080/02786820500182040.
Ervens, B., Turpin, B.J., Weber, R.J., 2011. Secondary organic aerosol formation in cloud droplets and aqueous particles (aqSOA): a review of laboratory, field and model studies. Atmos. Chem. Phys. 11, 11069–11102. https://doi.org/10.5194/acp-11-11069-2011.
Farmer, D.K., Matsunaga, A., Docherty, K.S., Surratt, J.D., Seinfeld, J.H., Ziemann, P.J., Jimenez, J.L., 2010. Response of an aerosol mass spectrometer to organonitrates and organosulfates and implications for atmospheric chemistry. Proc. Natl. Acad. Sci. U. S. A. 107, 6670–6675. https://doi.org/10.1073/pnas.0912340107.
Fry, J.L., Draper, D.C., Zarzana, K.J., Campuzano-Jost, P., Day, D. a., Jimenez, J.L., Brown, S.S., Cohen, R.C., Kaser, L., Hansel, a., Cappellin, L., Karl, T., Hodzic Roux, a., Turnipseed, a., Cantrell, C., Lefer, B.L., Grossberg, N., 2013. Observations of gas- and aerosol-phase organic nitrates at BEACHON-RoMBAS 2011. Atmos. Chem. Phys. 13, 8585–8605. https://doi.org/10.5194/acp-13-8585-2013.
Fry, J.L., Kiendler-Scharr, A., Rollins, A.W., Wooldridge, P.J., Brown, S.S., Fuchs, H., Dubé, W., Mensah, A., dal Maso, M., Tillmann, R., Dorn, H.-P., Brauers, T., Cohen, R.C., 2009. Organic nitrate and secondary organic aerosol yield from NO3 oxidation of β-pinene evaluated using a gas-phase kinetics/aerosol partitioning model. Atmos. Chem. Phys. 9, 1431–1449. https://doi.org/10.5194/acp-9-1431-2009.
Gaur, A., Tripathi, S.N., Kanawade, V.P., Tare, V., Shukla, S.P., 2014. Four-year measurements of trace gases (SO2, NOx, CO, and O3) at an urban location, Kanpur, in Northern India. J. Atmos. Chem. 71, 283–301. https://doi.org/10.1007/s10874-014-9295-8.
Gilardoni, S., Massoli, P., Giulianelli, L., Rinaldi, M., Paglione, M., Pollini, F., Lanconelli, C., Poluzzi, V., Carbone, S., Hillamo, R., Russell, L.M., Facchini, M.C., Fuzzi, S., 2014. Fog scavenging of organic and inorganic aerosol in the Po Valley. Atmos. Chem. Phys. 14, 6967–6981. https://doi.org/10.5194/acp-14-6967-2014.
Gilardoni, S., Massoli, P., Paglione, M., Giulianelli, L., Carbone, C., Rinaldi, M., Decesari, S., Sandrini, S., Costabile, F., Gobbi, G.P., Pietrogrande, M.C., Visentin, M., Scotto, F., Fuzzi, S., Facchini, M.C., 2016. Direct observation of aqueous secondary organic aerosol from biomass-burning emissions. Proc. Natl. Acad. Sci. U. S. A. 113, 10013–10018. https://doi.org/10.1073/pnas.1602212113.
Hallquist, M., Wenger, J.C., Baltensperger, U., Rudich, Y., Simpson, D., Claeys, M., Dommen, J., Donahue, N.M., George, C., Goldstein, A.H., Hamilton, J.F., Herrmann, H., Hoffmann, T., Iinuma, Y., Jang, M., Jenkin, M.E., Jimenez, J.L., Kiendler-Scharr, A., Maenhaut, W., McFiggans, G., Mentel, T.F., Monod, A., Prévôt, A.S.H., Seinfeld, J.H., Surratt, J.D., Szmigielski, R., Wildt, J., 2009. The formation, properties and impact of secondary organic aerosol: current and emerging issues. Atmos. Chem. Phys. 9, 5155–5236.
Heald, C.L., Kroll, J.H., Jimenez, J.L., Docherty, K.S., Decarlo, P.F., Aiken, A.C., Chen, Q., Martin, S.T., Farmer, D.K., Artaxo, P., 2010. A simplified description of the evolution of organic aerosol composition in the atmosphere. Geophys. Res. Lett. 37 https://doi.org/10.1029/2010GL042737.
Jimenez, J.L., Canagaratna, M.R., Donahue, N.M., Prévôt, A.S.H., Zhang, Q., Kroll, J.H., DeCarlo, P.F., Allan, J.D., Coe, H., Ng, N.L., Aiken, A.C., Docherty, K.S., Ulbrich, I.M., Grieshop, A.P., Robinson, A.L., Duplissy, J., Smith, J.D., Wilson, K.R., Lanz, V.A., Hueglin, C., Sun, Y.L., Tian, J., Laaksonen, A., Raatikainen, T., Rautiainen, J., Vaattovaara, P., Ehn, M., Kulmala, M., Tomlinson, J.M., Collins, D.R., Cubison, M.J., Dunlea, E.J., Huffman, J.A., Onasch, T.B., Alfarra, M.R., Williams, P.I., Bower, K., Kondo, Y., Schneider, J., Drewnick, F., Borrmann, S., Weimer, S., Demerjian, K., Salcedo, D., Cottrell, L., Griffin, R., Takami, A., Miyoshi, T., Hatakeyama, S., Shimono, A., Sun, J.Y., Zhang, Y.M., Dzepina, K., Kimmel, J.R., Sueper, D., Jayne, J.T., Herndon, S.C., Trimborn, A.M., Williams, L.R., Wood, E.C., Middlebrook, A.M., Kolb, C.E., Baltensperger, U., Worsnop, D.R., 2009. Evolution of organic aerosols in the atmosphere. Science 326, 1525–1529. https://doi.org/10.1126/science.1180353.
Kanawade, V.P., Tripathi, S.N., Bhattu, D., Shamjad, P.M., 2014. Sub-micron particle number size distributions characteristics at an urban location, Kanpur, in the Indo-Gangetic Plain. Atmos. Res. 147–148, 121–132. https://doi.org/10.1016/j.atmosres.2014.05.010.
Kang, E., Toohey, D.W., Brune, W.H., 2011. Dependence of SOA oxidation on organic aerosol mass concentration and OH exposure: experimental PAM chamber studies. Atmos. Chem. Phys. 11, 1837–1852. https://doi.org/10.5194/acp-11-1837-2011.
Kaul, D.S., Gupta, T., Tripathi, S.N., Tare, V., Collett Jr., J.L., 2011. Secondary organic aerosol: a comparison between foggy and nonfoggy days. Environ. Sci. Technol. 45, 7307–7313. https://doi.org/10.1021/es201081d.
Kroll, J.H., Smith, J.D., Che, D.L., Kessler, S.H., Worsnop, D.R., Wilson, K.R., 2009. Measurement of fragmentation and functionalization pathways in the heterogeneous oxidation of oxidized organic aerosol. Phys. Chem. Chem. Phys. 11, 8005–8014. https://doi.org/10.1039/b905289e.
Kumar, A., Gupta, T., 2015. Development and laboratory performance evaluation of a variable configuration PM1/PM2.5 impaction-based sampler. Aerosol Air Qual. Res. 15, 768–775. https://doi.org/10.4209/aaqr.2014.11.0307.
Lanz, V.A., Alfarra, M.R., Baltensperger, U., Buchmann, B., Hueglin, C., Prévôt, A.S.H., 2007. Source apportionment of submicron organic aerosols at an urban site by factor analytical modelling of aerosol mass spectra. Atmos. Chem. Phys. 7, 1503–1522.
Liu, S., Shilling, J.E., Song, C., Hiranuma, N., Zaveri, R.A., Russell, L.M., 2012. Hydrolysis of organonitrate functional groups in aerosol particles. Aerosol Sci. Technol. 46, 1359–1369. https://doi.org/10.1080/02786826.2012.716175.
Middlebrook, A.M., Bahreini, R., Jimenez, J.L., Canagaratna, M.R., 2012. Evaluation of composition-dependent collection efficiencies for the aerodyne aerosol mass spectrometer using field data. Aerosol Sci. Technol. 46, 258–271. https://doi.org/10.1080/02786826.2011.620041.
Ng, N.L., Canagaratna, M.R., Jimenez, J.L., Chhabra, P.S., Seinfeld, J.H., Worsnop, D.R., 2011. Changes in organic aerosol composition with aging inferred from aerosol mass spectra. Atmos. Chem. Phys. 11, 6465–6474. https://doi.org/10.5194/acp-11-6465-2011.
Petit, J.-E., Favez, O., Albinet, A., Canonaco, F., 2017. A user-friendly tool for comprehensive evaluation of the geographical origins of atmospheric pollution: wind and trajectory analyses. Environ. Model. Softw. 88, 183–187. https://doi.org/10.1016/j.envsoft.2016.11.022.
Pfaffenberger, L., Barmet, P., Slowik, J.G., Praplan, A.P., Dommen, J., Prévôt, A.S.H., Baltensperger, U., 2013. The link between organic aerosol mass loading and degree of oxygenation: an α-pinene photooxidation study. Atmos. Chem. Phys.

13, 6493–6506. https://doi.org/10.5194/acp-13-6493-2013.
Rai, P., Chakraborty, A., Mandariya, A.K., Gupta, T., 2016. Composition and source apportionment of PM1 at urban site Kanpur in India using PMF coupled with CBPF. Atmos. Res. 178–179, 506–520. https://doi.org/10.1016/j.atmosres.2016.04.015.
Rajput, P., Sarin, M.M., 2014. Polar and non-polar organic aerosols from large-scale agricultural-waste burning emissions in Northern India: implications to organic mass-to-organic carbon ratio. Chemosphere 103, 74–79. https://doi.org/10.1016/j.chemosphere.2013.11.028.
Rajput, P., Sarin, M.M., Rengarajan, R., Singh, D., 2011. Atmospheric polycyclic aromatic hydrocarbons (PAHs) from post-harvest biomass burning emissions in the Indo-Gangetic Plain: isomer ratios and temporal trends. Atmos. Environ. 45, 6732–6740. https://doi.org/10.1016/j.atmosenv.2011.08.018.
Ram, K., Tripathi, S.N., Sarin, M.M., Bhattu, D., 2014. Primary and secondary aerosols from an urban site (Kanpur) in the Indo-Gangetic Plain: impact on CCN, CN concentrations and optical properties. Atmos. Environ. 89, 655–663. https://doi.org/10.1016/j.atmosenv.2014.02.009.
Rastogi, N., Singh, A., Singh, D., Sarin, M.M., 2014. Chemical characteristics of PM2.5 at a source region of biomass burning emissions: evidence for secondary aerosol formation. Environ. Pollut. 184, 563–569. https://doi.org/10.1016/j.envpol.2013.09.037.
Salcedo, D., Onasch, T.B., Dzepina, K., Canagaratna, M.R., Zhang, Q., Huffman, J.A., DeCarlo, P.F., Jayne, J.T., Mortimer, P., Worsnop, D.R., Kolb, C.E., Johnson, K.S., Zuberi, B., Marr, L.C., Volkamer, R., Molina, L.T., Molina, M.J., Cardenas, B., Bernabe, R.M., Marquez, C., Gaffney, J.S., Marley, N.A., Laskin, A., Shutthanandan, V., Xie, Y., Brune, W., Lesher, R., Shirley, T., Jimenez, J.L., 2006. Characterization of ambient aerosols in Mexico city during the MCMA-2003 campaign with aerosol mass spectrometry: results from the CENICA supersite. Atmos. Chem. Phys. 6, 925–946.
Schurman, M.I., Lee, T., Sun, Y., Schichtel, B.A., Kreidenweis, S.M., Collett Jr., J.L., 2015. Investigating types and sources of organic aerosol in Rocky Mountain National Park using aerosol mass spectrometry. Atmos. Chem. Phys. 15, 737–752. https://doi.org/10.5194/acp-15-737-2015.
Shilling, J.E., Chen, Q., King, S.M., Rosenoern, T., Kroll, J.H., Worsnop, D.R., DeCarlo, P.F., Aiken, a. C., Sueper, D., Jimenez, J.L., Martin, S.T., 2009. Loading-dependent elemental composition of α-pinene SOA particles. Atmos. Chem. Phys. 9, 771–782.
Takegawa, N., Miyakawa, T., Kondo, Y., Blake, D.R., Kanaya, Y., Koike, M., Fukuda, M., Komazaki, Y., Miyazaki, Y., Shimono, A., Takeuchi, T., 2006a. Evolution of submicron organic aerosol in polluted air exported from Tokyo. Geophys. Res. Lett. 33 https://doi.org/10.1029/2006gl025815.
Takegawa, N., Miyakawa, T., Kondo, Y., Jimenez, J.L., Zhang, Q., Worsnop, D.R., Fukuda, M., 2006b. Seasonal and diurnal variations of submicron organic aerosol in Tokyo observed using the Aerodyne aerosol mass spectrometer. J. Geophys. Res. 111 https://doi.org/10.1029/2005jd006515.
Takegawa, N., Miyakawa, T., Watanabe, M., Kondo, Y., Miyazaki, Y., Han, S., Zhao, Y., van Pinxteren, D., Bruggemann, E., Gnauk, T., Herrmann, H., Xiao, R., Deng, Z., Hu, M., Zhu, T., Zhang, Y., 2009. Performance of an aerodyne aerosol mass spectrometer (AMS) during intensive campaigns in China in the summer of 2006. Aerosol Sci. Technol. 43, 189–204. https://doi.org/10.1080/02786820802582251.
Takegawa, N., Miyazaki, Y., Kondo, Y., Komazaki, Y., Miyakawa, T., Jimenez, J.L., Jayne, J.T., Worsnop, D.R., Allan, J.D., Weber, R.J., 2005. Characterization of an aerodyne aerosol mass spectrometer (AMS): intercomparison with other aerosol instruments. Aerosol Sci. Technol. 39, 760–770. https://doi.org/10.1080/02786820500243404.
Tripathi, S.N., Tare, V., Chinnam, N., Srivastava, A.K., Dey, S., Agarwal, A., Kishore, S., Lal, R.B., Manar, M., Kanwade, V.P., Chauhan, S.S.S., Sharma, M., Reddy, R.R., Gopal, K.R., Narasimhulu, K., Reddy, L.S.S., Gupta, S., Lal, S., 2006. Measurements of atmospheric parameters during indian space research organization geosphere biosphere programme land campaign ii at a typical location in the ganga basin: 1. Physical and optical properties. J. Geophys. Res. Atmos. 111 https://doi.org/10.1029/2006JD007278.
Ulbrich, I.M., Canagaratna, M.R., Zhang, Q., Worsnop, D.R., Jimenez, J.L., 2009. Interpretation of organic components from Positive Matrix Factorization of aerosol mass spectrometric data. Atmos. Chem. Phys. 9, 2891–2918.
Zhang, Q., Alfarra, M.R., Worsnop, D.R., Allan, J.D., Coe, H., Canagaratna, M.R., Jimenez, J.L., 2005. Deconvolution and quantification of hydrocarbon-like and oxygenated organic aerosols based on aerosol mass spectrometry. Environ. Sci. Technol. 39, 4938–4952. https://doi.org/10.1021/es048568l.
Zhang, Q., Jimenez, J.L., Canagaratna, M.R., Allan, J.D., Coe, H., Ulbrich, I., Alfarra, M.R., Takami, A., Middlebrook, A.M., Sun, Y.L., Dzepina, K., Dunlea, E., Docherty, K., DeCarlo, P.F., Salcedo, D., Onasch, T., Jayne, J.T., Miyoshi, T., Shimono, A., Hatakeyama, S., Takegawa, N., Kondo, Y., Schneider, J., Drewnick, F., Borrmann, S., Weimer, S., Demerjian, K., Williams, P., Bower, K., Bahreini, R., Cottrell, L., Griffin, R.J., Rautiainen, J., Sun, J.Y., Zhang, Y.M., Worsnop, D.R., 2007. Ubiquity and dominance of oxygenated species in organic aerosols in anthropogenically-influenced Northern Hemisphere midlatitudes. Geophys. Res. Lett. 34 https://doi.org/10.1029/2007gl029979.
Zhang, Y., Tang, L., Croteau, P.L., Favez, O., Sun, Y., Canagaratna, M.R., Wang, Z., Couvidat, F., Albinet, A., Zhang, H., Sciare, J., Prévôt, A.S.H., Jayne, J.T., Worsnop, D.R., 2017. Field characterization of the PM_{2.5} Aerosol Chemical Speciation Monitor: insights into the composition, sources and processes of fine particles in Eastern China. Atmos. Chem. Phys. Discuss. 1–52. https://doi.org/10.5194/acp-2017-233.